N68-12494

(ACCESSION NUMBER)

_26_
(PAGES)

(THRU)

(CODE)

(NASA CR OR TMX OR AD NUMBER)

(CATEGORY)

FF No. 602(C)

TRANSIENT BEHAVIOR OF ARTERIAL SYSTEMS IN RESPONSE TO FLOW PULSES

by E. D. Young

Prepared by
GENERAL TECHNICAL SERVICES, INC.
Upper Darby, Pa.
for

TRANSIENT BEHAVIOR OF ARTERIAL SYSTEMS

IN RESPONSE TO FLOW PULSES

By E. D. Young

Distribution of this report is provided in the interest of
information exchange.   Responsibility for the contents
resides in the author or organization that prepared it.

NATIONAL AERONAUTICS AND SPACE ADMINISTRATION

FOREWORD

This report is the sixth technical report under the present contract and the ninth in a series. The general aim of the program is to develop models adequate to account for the dynamic characteristics of selected systems in mammals.

Continuing the general aim this report provides a theory of the arterial pulse in what appears to be an exceptionally neat form, since it characterizes the responses of the system in terms of transformations which may be graphed by hand and easily visualized. This should provide a solid foundation for the use of pulse wave techniques in diagnosis.

The problem was undertaken under the general supervision of the program director, A. Iberall. This report is the more detailed exposition of introductory material presented at the November 1966 Annual Conference on Engineering in Medicine and Biology in San Francisco.

TABLE OF CONTENTS

INTRODUCTION

Analyses of transmission in arterial trees has generally fallen into one of three categories:

1. Transient analyses

2. Fourier analyses

3. Analog simulation

The earlier investigators in the field viewed the inputs to the system in terms of isolated "pulses" (individual heart beats). Their discussion was basically phrased in terms of simple physical models, e.g., the windkessel of Frank. An extensive bibliography is contained in (15). Later (due to the influence of Womersley), Fourier decomposition became the mode of investigation for nearly everyone with the exception of J. Malcolm (who validly attempted to model the entire system albeit with a distorted view of the heart oscillator), Noordergraaf (17) and Taylor (23), whose investigations admit to a continuous spectrum.

Womersley (26) discussed the response of a straight arterial segment quite thoroughly. Actually, similar discussion was begun by Witzig (25), but this effort lapsed into obscurity. Noordergraaf deals with the straight arterial segment, by a sequence of delay line circuit models, each successive model dealing with a broader spectrum of inputs. The larger segments are then connected in a fashion suggested by gross anatomy, but not actually representative of anatomy, and the terminal impedances are anticipated as resistive. Taylor (22) has done numerous digital calculations of the impedance of random arrays of branching systems made up of straight segments.

Other analyses of the system as a whole tend to consider it "equivalent" to some ideal system with regular geometry which may be easily analyzed - especially at the lower end. Early attempts of this kind include the several lumped systems of Karreman (13) and later the regular geometry was replaced by a continuous tapered model (9), (19), (5). Iberall (9) discusses its anatomical justification.

In any case, there is a three-fold systems problem:

1. the problem of straight tube transmission,

2. the problem of terminal impedance,

3. the problem of dealing with transmission across a region of gross branching which is somewhat regular.

In this paper we hope to:

1. show the relation of transient analysis of fluid lines to harmonic analysis thereof,

2. indicate the practicality of formulating the transmission problem with respect to transients in the time domain and uniformly with respect to "frequency" or pulse width within the domain of linearity assumptions of Witzig (25), Iberall (8), Womersley (26), etc.

3. apply this transient analysis to a whole class of systems embracing in principle the normal range of mammalian arterial systems, which should help to clarify the meaning of "equivalence" among various idealized models mentioned.

4. trace causal relations between familiar wave distortions seen in arterial trees (see MacDonald (16)) and the basic geometry of the trees, or that of the equivalent systems.

Heretofore, data concerning normal geometry of the arterial system has been adapted from Green (6). This has been modified by Iberall (10). The following table is taken from (10). The table shows:

1. An organization into "levels", the first level being the aorta, the second consisting of all its branches, the third consisting of all branches of these, etc.

2. A graduation of size, with some overlapping which is initiated at first level by the variation in size of organs fed.

3. A preservation of total cross-sectional area over the first three levels.

4. A subsequent increase in cross-sectional area according to a rule for branching diameters, $d^k = \Sigma d_n^k$ where d's are diameters and where k increases to 2.7 from the fourth level. Suwa et al (21) give data showing a general nearly linear correlation of arterial segment length, ℓ, with diameter, d, its constant depending somewhat on the tissue examined. The values for ℓ/d are generally between 5 and 30 (practically never below 3).

These properties will be stated again as a formal arterial model, except that for the purpose of clarity, the overlapping and occasional wide deviation of ℓ/d will be minimized. This makes no difference in the results found.

2

Level No.	Diameter - cm Ent.	Diameter - cm Exit	Diameter - cm Ent. (av.)	Area - cm² Total for the Level	Area - cm² Ent (av.)	Area - cm² Exit	No. of Tubes	Groat-Suwa expon.
1	2.0	0.7	2.0	3.2	3.2	0.35	1	
2	1.0-.18	.18	.47	3.4	.17	.026	20	2
3	.4-.1	.1	.13	3.4	.013	.008	260	
4	.2-.04	.04	.08	4.0	.005	1.3×10^{-3}	800	2
5	.08-.02	.02	.031	5	7.6×10^{-4}	3.0×10^{3}	7×10^{3}	2.7
6	.04-.01	.01	.016	6	1.9×10^{-4}	8.0×10^{-5}	3×10^{4}	2.7
7	.02-.004	.004	.008	10	4.8×10^{-5}	1.3×10^{-5}	2×10^{5}	2.7
8	.01-.0025	.0025	.0032	16	7.6×10^{-6}	5.0×10^{-6}	2×10^{6}	2.7
9	.006-.0015	.0015	.0020	25	3.0×10^{-6}	1.8×10^{-6}	8×10^{6}	2.7
10	.003-.0008	.0008	.0012	35	1.1×10^{-6}	5.0×10^{-7}	3×10^{7}	2.7
11	.0015-.0004	.0004	.0008	80	5.0×10^{-7}	5.0×10^{-7}	2×10^{8}	large

ESTIMATED ARTERIAL TREE GEOMETRY AND RESISTANCE FOR 23 kg DOG

MATHEMATICAL APPARATUS

In considering transient behavior of fluid lines we restrict our attention to the class of functions of a real variable t (t will represent time) having Fourier transforms; being continuous; having only a finite number of maxima and minima; and being also such that $f(t) = 0$ for $t < a$, a being some real number. In discussing such functions we shall encounter transformations defined by

$$T(f) = F^{-1}(g \cdot F(f))$$

i. e., by

$$F(T(f)) = (g \cdot F(f))$$

where F denotes the Fourier transform and g is some complex valued function of a real variable ω.

The function g must, in general, have the property that $g(-\omega) = g*(\omega)$ where the asterisk denotes the complex conjugate. Transformations described in this way are necessarily linear and the function g then is a representation of the transformation T. Further, if g_1 represents T_1 and g_2 represents T_2, then

1. $g_1 + g_2$ represents the transform $T_1 + T_2$ where $T_1 + T_2$ is defined so that $(T_1 + T_2)f = T_1(f) + T_2(f)$ and

2. $g_1 \cdot g_2 = g_2 \cdot g_1$ represents $T_1 \cdot T_2 = T_2 \cdot T_1$

where

$$(T_1 \cdot T_2) f = T_1(T_2(f)).$$

Also in case there is a function k such that $F(k) = g$ where g represents T, then from the so-called folding theorem

$$F^{-1} (g \cdot F(f)) = k * f$$

i.e.,

$$T(f) = k * f$$

where k * f is the function h defined by

$$h(t) = \int_0^\infty k(t-u) f(u) du.$$

The function h is called the convolution of k and f. This means that the transformation T may also be represented in another sense by the kernel function k and may be applied to f by performing the convolution. Since convolution is not altogether difficult to visualize, we favor transformations with the kernel representation in this analysis.

In fact, in order to show that F^{-1} (g $\cdot$ F(f)) exists for the g's involved in transmission lines, we restrict the domain of allowable functions to those of form

$$f = k * h$$

where h is transformable and

$$k = F^{-1} (e^{-k(j\omega)^{2/3}})$$

for some real number k. However, if k is small then f is graphically indistinguishable from h so that the restriction is theoretically significant but not a practical one.

APPLICATION TO FLUID LINE PROBLEMS

For a straight segment of fluid filled elastic tube the one-dimensional aspect of the transmission problem is determined by the equations:

$$ZF(Q) = -\frac{\partial F(P)}{\partial x}$$

$$YF(P) = -\frac{\partial F(Q)}{\partial x} \tag{1}$$

(c.f. (4)) where Q is flow, P is pressure, these being functions of distance, x, and time, t. The variable Z is called the line impedance; Y is called the shunt admittance, these being complex valued functions of the frequency, ω. F is the Fourier transform, which, for functions of two variables, is defined by

$$F(f) = g$$

$$g(\omega,x) = \int_{-\infty}^{\infty} f(t,x)\, e^{j\omega t}\, dt.$$

One easily derives the relation between the vectors at two points, x_1, x_2.

$$\begin{bmatrix} q(\omega,x_2) \\ p(\omega,x_2) \end{bmatrix} = \begin{bmatrix} \cosh\left(\sqrt{Y(\omega)Z(\omega)}\,\triangle(X)\right) & \sqrt{\frac{Y(\omega)}{Z(\omega)}}\,\sinh\left(\sqrt{Y(\omega)Z(\omega)}\triangle x\right) \\ \sqrt{\frac{Z(\omega)}{Y(\omega)}}\,\sinh\left(\sqrt{Y(\omega)Z(\omega)}\triangle x\right) & \cosh\left(\sqrt{Y(\omega)Z(\omega)}\triangle x\right) \end{bmatrix} \begin{bmatrix} q(\omega,x_1) \\ p(\omega,x_1) \end{bmatrix} \tag{2}$$

where

$$q = F(Q), p = F(P).$$

The matrix involved is called the chain matrix (24). If we regard (Q,P), (q,p) as families of real valued or complex valued functions indexed by the values of the continuous variable x then we may write the above as

$$\begin{bmatrix} q_{x_2} \\ p_{x_2} \end{bmatrix} = \begin{bmatrix} \cosh(\sqrt{YZ}\,\triangle x) & \sqrt{\frac{Y}{Z}}\,\sinh\sqrt{YZ}\,\triangle x \\ \sqrt{\frac{Z}{Y}}\,\sinh(\sqrt{YZ}\,\triangle x) & \cosh(\sqrt{YZ}\,\triangle x) \end{bmatrix} \begin{bmatrix} q_{x_1} \\ p_{x_1} \end{bmatrix} \tag{2}$$

Now, Z Y are given formally in (25, 8, 26).

Explicitly

$$\sqrt{Y(\omega)Z(\omega)}\ \Delta x\ =\ \frac{t_o}{t_1}\ jz\left(1 - \frac{2J_1(\sqrt{-jz})}{\sqrt{-jz}J_o(\sqrt{-jz})}\right)^{-1/2} \tag{3}$$

$$\sqrt{\frac{Z(\omega)}{Y(\omega)}}\ =\ \frac{\rho c}{A}\left(1 - \frac{2J_1(\sqrt{-jz})}{\sqrt{-jz}J_o(\sqrt{-jz})}\right)^{-1/2}$$

where

$c\ =$ propagation velocity (Moens-Korteweg velocity for arteries).

$t_o\ =\ \dfrac{\Delta x}{c}$

$\Delta x\ =$ distance along the tube

$t_1\ =\ \dfrac{r^2}{\nu}$

$\nu\ =$ kinematic viscosity of the fluid

$r\ =$ tube radius (interior)

$z\ =\ \omega t_1$

$\rho\ =$ fluid density

$A\ =$ cross sectional area of the tube

J_o, J_1 are Bessel functions

$j\ =\ \sqrt{-1}$

One may verify that

$$\sqrt{Y(\omega)Z(\omega)}\Delta x\ =\ \frac{t_o}{t_1}\ (jz + \epsilon(z))$$

7

where the function ϵ is characterized by the existence of an inverse transform

$$F^{-1}\left(e^{-t_o/t_1 \epsilon(z)}\right) = K_a$$

which is a kernel function. Thus $e^{-\sqrt{YZ}\,\Delta x}$ represents the product of a "translation" in time to T_{to} where if $h = T_{to}(f)$ then $h(t) = f(t+t_o)$ and a transform Ta where $T_a(f) = K_a * f$. To the first order the graph of K_a is given in figure 1 for the case where $t_o/t_1 = 1$.

Further $\sqrt{Y/Z}$ represents a transform of form $A/\rho c\left[I - T_{t1}\right]$ where I is identity i.e. $I(f) = f$ and $T_{t1}(f) = K_{t1} * f$. K_{t1} is represented in figure 2. A method of calculation is given in Appendix A.

In summary, for a straight fluid filled tube specified by the parameter t_o/t_1, $\rho c/A$, t_1 the relationship of the flow Q_{x1}, and pressure P_{x1}, at station x_1, to the corresponding pair at station x_2 are given by

$$\begin{bmatrix} Q_{x2} \\ P_{x2} \end{bmatrix} = \begin{bmatrix} C_a & Z_b^{-1} S_a \\ Z_b S_a & C_a \end{bmatrix} \begin{bmatrix} Q_{x1} \\ P_{x1} \end{bmatrix} \tag{4}$$

where

$$C_a = \frac{T_{to} T_a + T_{to}^{-1} T_a^{-1}}{2}$$

$$S_a = \frac{T_{to} T_a - T_{to}^{-1} T_a^{-1}}{2}$$

$$Z_b = \frac{\rho c}{A}(I - T_{t1})^{-1}$$

T_{to}, T_a, T_{t1}, are the transforms previously mentioned which are applied by convolution with their kernel representations.

We remark that the transformation given in equation 4 has a set of eigen vectors representing propagation in an infinite tube or one with matched termination. The eigen vectors are pairs of the form

$$\left(Q, \frac{\rho c}{A}(I - T_{t1})^{-1} Q\right)$$

i.e., $(Q, Z_b Q)$. The "eigen values" however are $T_a T_a^{-1}$.

8

APPLICATION TO A CLASS OF NETWORKS
SIMILAR TO ARTERIAL TREES

The formal definition of the class described in the introduction is as follows:

The class consists of fluid filled labyrinths, each consisting of straight tube segments joined together to form a multi-level structure. The first level consists of a single progression of tube segments whose members are non-increasing in diameter. Each segment of the progression terminates at the beginning of two other segments of the system. If the ratio of the diameters of the latter pair is less than .85, then the larger of the pair is counted as next in the progression -- otherwise the progression is terminated. If the labyrinth contains at least three levels, then each tube involved in the termination of a member of the progression is the first tube in a new progression -- each of which (progression) belongs to the second and last level of the system. If the labyrinth contains at least four levels then each tube involved in the termination of a segment of a second level progression is the beginning of a third level progression. The progressions in a labyrinth will be termed arteries, and the progressions beginning at the termini of members of a progression will be called its tributaries. While somewhat strange, perhaps - upon careful study of the formalism - it will be found to be quite adequate and natural as a description of the actual characteristics of arterial trees for the most part.)

Furthermore the tributaries of an artery have the following regularities:

1. At the mouth of a tributary, if d_n is the diameter of the nth segment, d_{n+1} is the diameter of the next segment, and d_t is the tributary diameter, then $d_n^k = d_{n+1}^k + d_t^k$ where $2 < k < 3$; or in case of a terminus, $d_n^k = d_{t1}^k$. For all arteries of the mth level, k has the same value and, further, is a non-decreasing function of m.

2. If ℓ_i is the length of the ith segment, then $5 < \ell_i/d_i < 25$.

3. If t_1 and t_2 are tributaries of the same artery having entrance diameters d_1 and d_2, then $.65 < d_1/d_2 < .65^{-1}$ (i.e., small tributaries are ignored).

4. The number of segments in an artery is between 4 and 12.

5. The density of the fluid is about 1 gm/cm^3; the kinematic viscosity is about .035 poise.

6. The propagation velocity is a non-decreasing function of the level ordinal, i.e., arteries of level m have velocity c_m and $c_{m+1} \gtrsim c_m$.

7. The first artery of the labyrinth has an entrance diameter of at least 1/2cm and a propagation velocity of $250 < c < 750$ cm/sec.

8. The last level consists of arteries of diameter less than 30 (μ). (The numerical values which were chosen are essentially suitable in a quantitative sense for actual trees. However, their precise magnitude and ranges are a matter of indifference).

To analyze the transient behavior of such a system, we begin with arteries of the next to last level. The arteries of the last level are characterized by an impedance transform Z_E where $P_E = Z_E$ Q_E. Working up from the bottom, it is theoretically possible to derive a driving point impedance law for each system whose main artery is of the order of 3mm in size.

In Appendix B we show that conservatively speaking any such subsystem of any of the systems under discussion may be replaced by a simple driving point impedance law, provided that the inputs to the subsystem are restricted to the convolution of functions of finite area with a function $\bar{K}$ given by

$$\bar{K} = F^{-1}(g), \quad g(\omega) = e^{(-1/3)\sqrt{j\omega}}$$

While the frequency restriction proposed is consistent with errors in wave form of not greater than a few per cent, an extension to high frequency content as high as 10 cps is tolerable, although with possible degradation of accuracy of the description. In any case, all the interesting inputs to a real arterial system are actually so filtered, that is, such details as the incisura are lost in transforming across the larger sized tube segments. Hence this is no restriction.

The impedance law is of the form (from Appendix B)

$$\left((\Sigma \frac{Vn}{\rho c_n^2}) D + A_E \right) P = (1+L)Q \tag{5}$$

where the summation in the expression is taken over the subsystems. D is the differential operator, A_E is the total of the d.c. admittance of the tributaries of the main (3mm) artery, L is a transform of small effect which represents the effect of momentum.

$$L = \sum_n \frac{R_n}{R_E} L_{t1}$$

where R_n is the d.c. resistance of the nth segment. R_E is the resistance of the terminal tributaries. L_{t1} (f) = (K_L) $_{t1}$ * f, where (K_L) $_{t1}$ is represented by

$$8(1-X)/jz$$

and

$$X(z) = \frac{2J_1(\sqrt{-jz})}{\sqrt{-jz} Jo \sqrt{-jz}}$$

A graph of (K_L) is shown in figure 3. The correction term as well as the volume term is normally small. Above the 3mm size, the termini of the arterial segments are sufficiently sparse to be of individual interest. The recursion

relations for Q_n, P_n are given by equation 4 composed with the tributary exit flow relation given by equation 5 (which defines $Z_{E,n}$ of figure 4). Thus the point to point calculation may be carried out graphically by simple convolutions with at most 3 families of kernel functions, K_a, K_{t1}, and $(K_L)t1$, corresponding to inverse transforms of

(1) $e^{-t_o/t_1 \epsilon(z)}$ where $\epsilon(z) = jz(-1+1/1-X)$ which is the convolution of $F^{-1}(e^{-\epsilon})$ with itself "t_o/t_1 times."

(2) $\delta = 1 - \sqrt{1-X}$

(3) $(1-X)/jz$ where $X(z) = \dfrac{2J_1(\sqrt{-jz})}{-\sqrt{jz}\, J_o(\sqrt{-jz})}$

which has an inverse transform K_x (figures 2, 3, 5).

We shall now apply the theory to a typical arterial system or subsystem, in particular a system consisting of an artery 25 cm long, 1/2 cm in diameter and terminating at a bifurcation into two 2mm sized labyrinths (figure 6).

The theory thus far can be used with extensive computation to test all sorts of interesting details of the response of an arterial system, or more casually and geometrically to produce salient information about it. The theory developed suffices to determine the unique response of the system to an arbitrary pressure pulse, introduced at its source, Pi, the response consisting of the flow pulses at the source and at the bifurcation, $Q_{r,o}$ and $Q_{r,1}$, respectively, together with the pressure pulse at the bifurcation, P_r.

To best illustrate the nature of the system's response, we shall assume a smooth pressure pulse as an input.

Now to calculate the response, it would suffice to express the driving point admittance transformation for the whole system and apply it to the input pressure pulse, Pi, to find the flow pulse at the source, $Q_{r,o}$; the chain matrix relation (equation 4) may then be used to compute P_r and $Q_{r,1}$.

However, a more instructive and succinct method of calculation will be used which, if carried to the ultimate, would proceed by successive "relaxations" of an initial guess for the terminal pressure, P_r. Actually, only one new approximation or "relaxation" will be sufficient to capture the nature of the system's response. The most instructive initial guess for P_r is taken to be the input pressure itself, namely P_i.

To make the example most pertinent, we assume

$$C = 250 cm/sec$$

so that

$$t_o \approx .1 \ sec, \quad t_1 \approx .75 \ sec \ (i.e., \ \tau = 1 \ corresponds \ to \ t = .75 \ sec).$$

(This might be an average value if the tube is somewhat tapered.) Furthermore, the calculations are carried out in dimensionless form. In dimensionless variables, the relation expressed by the chain matrix (equation 4) reduces to

$$\bar{Q}_o = C_a \bar{Q}_1 - (I - T_{t1}) S_a \bar{P}_1 \tag{6}$$

$$\bar{P}_o = \frac{-S_a}{I - T_{t1}} \bar{Q}_1 + C_a \bar{P}_1$$

Where

$$\bar{Q} = \frac{Q}{AC}, \quad \bar{P} = \frac{P}{\rho C^2}$$

and C_a, S_a involve phase lags of 0.1 sec. The transform T_{t1} corresponds to K_{t1} of figure 2, where unity on the abscissa corresponds to $t = .75$ sec.

Figure 7 shows a pair chosen according to the terminal impedance relation, equation 5 (referring to station 1, figure 6). Figure 8 shows the corresponding pair $\bar{Q}_o'$, $\bar{P}_o'$, which one would obtain at station 0 (figure 6) <u>if the arterial segment behaved as a pure inductive-capacitive transmission line.</u> We note the absence of the dicrotic waves or any particular steepening of wave front. This is to be compared to the correct pair, $\bar{Q}_o$, $\bar{P}_o$, for the fluid system to be exhibited in figure 12.

In order to trace the sources of distortion, we introduce the intermediary $\bar{Q}$ which defines the undistorted portion of $\bar{Q}_1$ in that the pair, $\bar{Q}$, $\bar{P}$ (involving the assumed terminal value, $\bar{P}_1$, shown in figure 9, is an "eigen vector" of the fluid line segment, being transmitted with "essentially" no distortion. The relation of $\bar{Q}$ to $\bar{P}_1$ is given by

$$\bar{Q} = (1 - T_{t1}) \bar{P}_1.$$

(In contrast, the eigen value pair for an L-C line is given by $\bar{Q} = \bar{P}_1$).

If $\bar{Q}_1$ and $\bar{Q}$ were equal, then there would be no distortion. This may be seen by substitution from the identity

$$\bar{Q}_1 = \bar{Q} + (\bar{Q}_1 - \bar{Q})$$

into the second of equations 6; and by noting that since the pair $\bar{Q}$, $\bar{P}_1$ is an eigen vector, then

$$T_a^{-1} \bar{P}_1 = \frac{-S_a}{1 - T_{t1}} Q + C_a \bar{P}_1.$$

Here, T_a^{-1} serves as an "eigen value," in that both components $\bar{Q}$ and $\bar{P}_1$ transform in an identical fashion -- specifically by the transformation T_a^{-1}, T_a, being an operator which accomplishes only slight smoothing of the pulse. (This explains the previous use of the word "essentially.") As it is $\bar{Q} \neq \bar{Q}_1$ and the difference $\bar{Q}_1 - \bar{Q}$ is acted on by the distortion operator $S_a(1-\underline{T}_{t1})^{-1}$, again from equations 6. Finally the result is added to the pressure $\bar{P}_1$, as a pressure distortion.

In a similar fashion, the additive transmissional distortion for flow is found using a corresponding eigen vector pair, $\bar{Q}_1$, $\bar{P}$, shown in figure 10.

Figure 11 shows $\bar{Q}_1$, $\bar{P}_1$ together with the additive distortions which are referred to as ϵ_q and $\bar{\epsilon}_p$. The sums are shown as $\bar{Q}_o$, $\bar{P}_o$ in figure 12. This figure already exhibits several familiar features seen in the actual arterial pulse pairs, e.g., the dicrotic wave and steepening in the rising ramp of pressure.

But, again, this calculation simply furnishes an exploratory point characteristic of the relation between terminal pressures, their corresponding terminal flows, and pressure-flow pairs at the source. From the systems point of view, the pulses labelled as $\bar{Q}_1$, $\bar{P}_1$ of figure 7 and $\bar{Q}_o$ of figure 12 constitute the response to the input pressure pulse labelled as $\bar{P}_o$ in figure 12.

To continue our illustration, let us assume that we wish to find the response of the system to the input pressure, $\bar{P}_i$, where $\bar{P}_i$ is the pulse labelled $\bar{P}_1$ in figure 7. We may obtain the response by finding what terminal pair $\bar{Q}_{r,1}$, $\bar{P}_r$ would, when transformed by the process just outlined, yield the given input pressure, $\bar{P}_1$. This could be done by a process of relaxation using the previous intermediate results.

Specifically, since the mismatch in impedance between the main tube and the terminal system is of second order, then to the first order, the solution for the pressure, $\bar{P}_r$, of our current problem is the difference between the input graph (shown as $\bar{P}_1$ in figure 11) and the graph marked ϵ_p in the same figure. Further corrections involve estimating that pressure curve which transforms into $-\epsilon_p$ by the process already outlined.

At any rate it is clear that the resulting pressure response at station 1 would involve the dicrotic wave and ramp steepening already noted.

SUMMARY

To summarize, let us survey the whole size range involved in an arterial tree of the class we have chosen to consider.

First, small subsystems involving only arteries appreciably smaller than 3mm may be represented by driving point impedances which are identical to a simple resistive-capacitive network, the individual segments behaving basically as lumped elements each contributing only slightly to the capacitance.

From this point up to the 3mm size, the individual elements no longer contribute inductance-free behavior, so that one has to begin paying attention to the changing character of the line impedance at a point below this level. The effect of the hybrid line impedance on the driving point impedance of a 3mm labyrinth is summarized in equation 5.

No detailed example of a calculation of the lumped network at this size has been given, although the impedance of the components is available from the line impedance and the chain matrix.

Immediately above the 3mm size, the effect of mismatching between the line impedance and the terminal impedance is evident from our example; for if they were equal, $\bar{Q}$ of figure 9 would be equal to $\bar{Q}_1$ of figure 7. In fact, the distortion of the calculated input pressure, ϵ_p of figure 11, is due to this mismatching in conjunction with the effect of the phase lag across the tube -- which at the level of this example is of the order of 0.1 sec.

Thus, it is hard to escape feeling that the peculiarity of the pulse transmission seen in arterial trees is well ascribed to the hybrid impedance nature of the fluid line segments in the system of the general dimensions considered in the example, i.e., one should expect the effects to be maximal in a zone where reflection from terminal or side tubes involves pulses of the same time width as twice the phase lag. From another view, these lines -- with reference to the pulse widths considered -- have a line impedance character which in contrast to the better matched inductive-capacitive line (see figure 8) involves "overshoots" in pressure and "undershoots" in flow which are reflected at the side branches.

Finally, arteries larger than .5 cm soon appear essentially inductive-capacitive in nature owing to the broadening of the kernel K_t to where its effect becomes negligible, except that there will be an erasure of high frequency or sharp detail because the filtering action represented by K_a (figure 1) becomes appreciable in any one segment or chain of segments for pulse widths of .05 sec when $\alpha = tt_1/t_o^2$ has a value of about 4 for $t > .05$, i.e., when $t_1/t_o^2 \approx 80$. Thus, the larger tubes restrict the possible detail to be dealt with in the smaller ones as noted earlier.

THE KERNEL K_a REPRESENTING PROPAGATIONAL DISTORTION FOR THE CASE WHERE $T_o/T_1 = 1$ TOGETHER WITH ITS EFFECT ON A TRIANGULAR PULSE
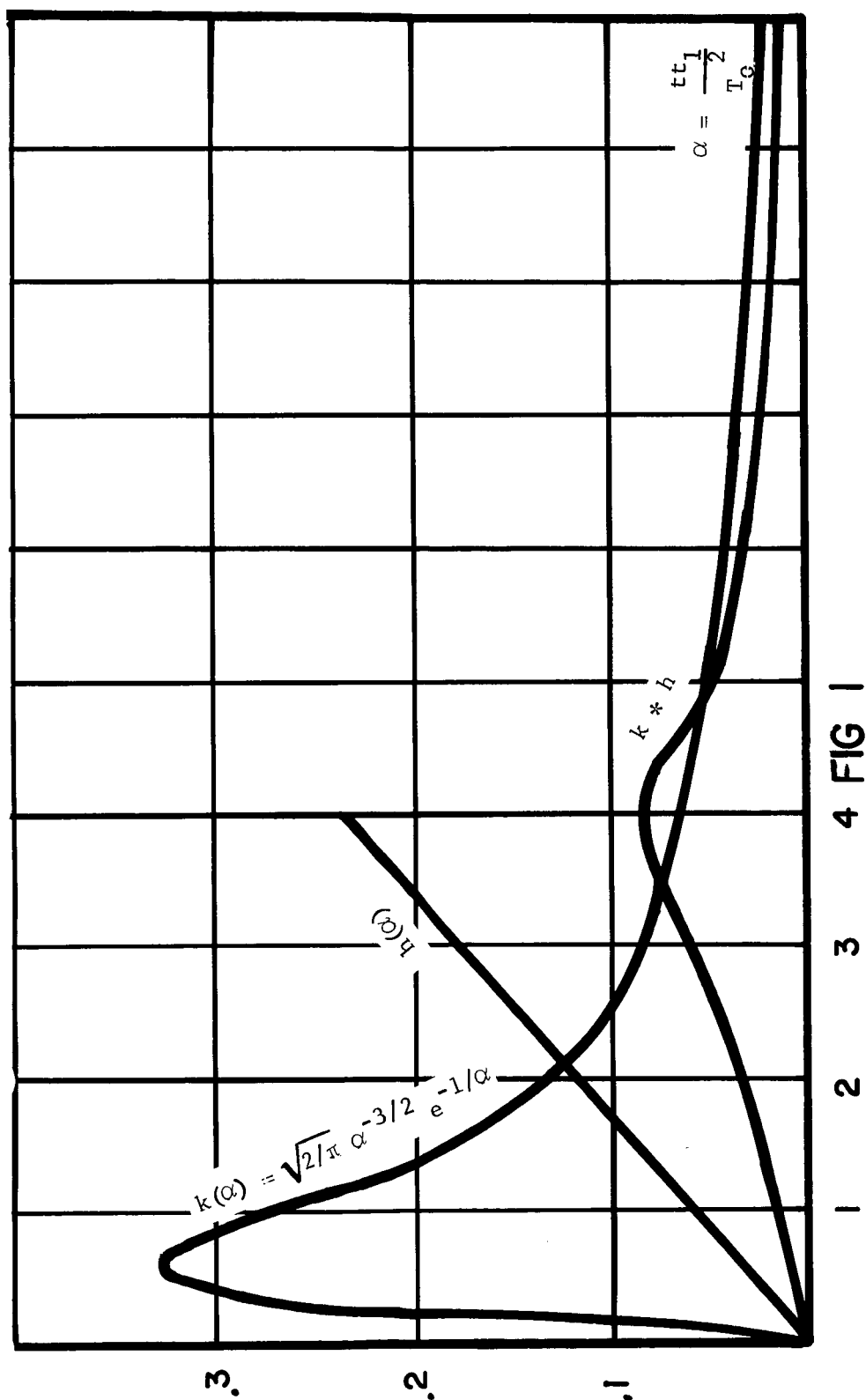

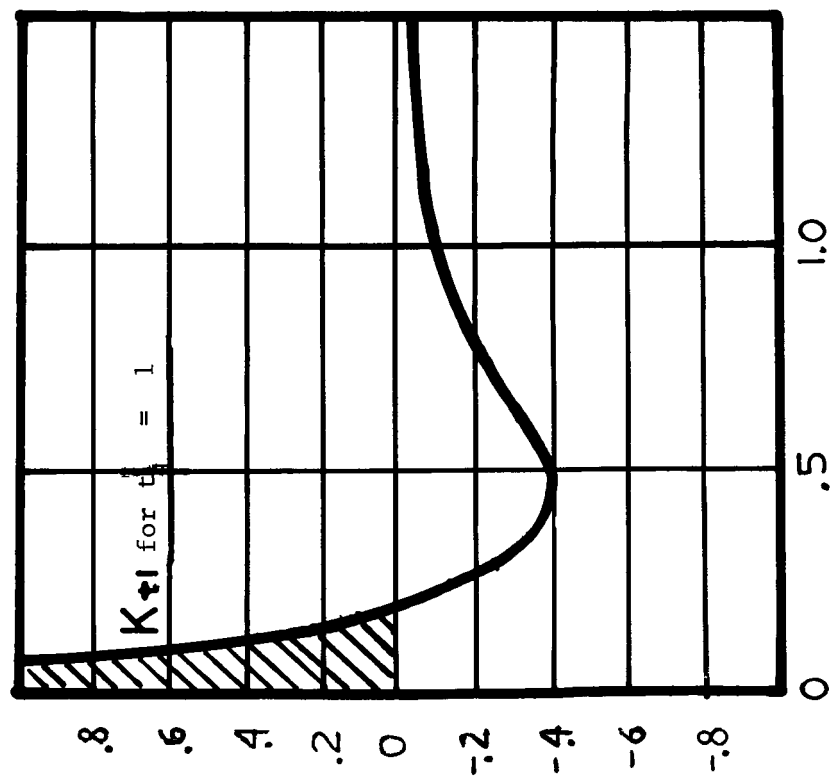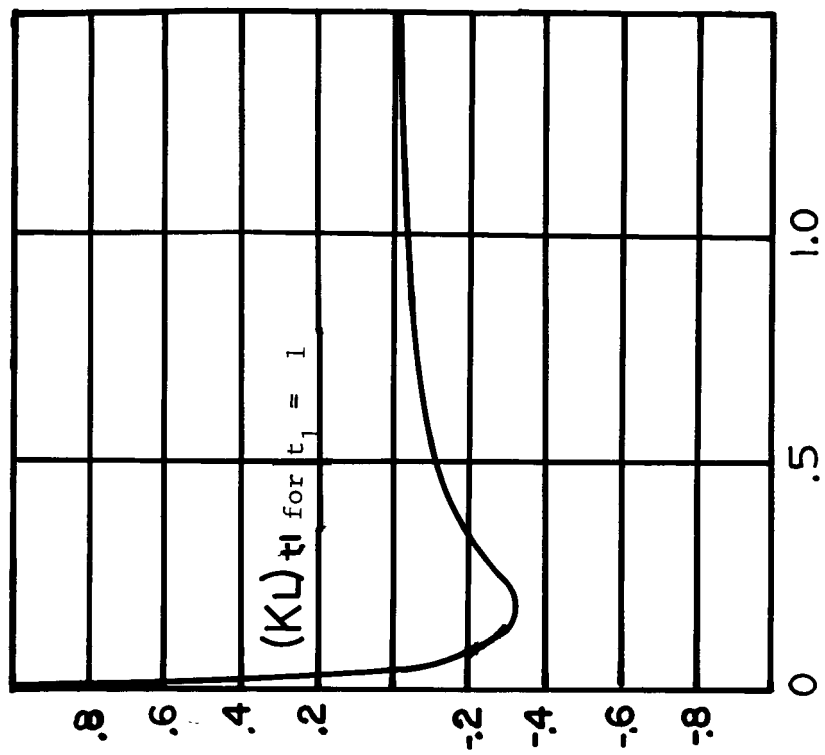$$k(\alpha) = \sqrt{2/\pi} \ \alpha^{-3/2} \ e^{-1/\alpha}$$

$h(\alpha)$

$k * h$

$$\alpha = \frac{t - t_{\frac{1}{2}}}{T_c}$$

FIG I

15

FIG 3

THE KERNEL $(K_L)_{t'}$

$(K_L)_{t'}$ for $t_1 = 1$

FIG 2

THE KERNEL $K_{t'}$

$K_{t'}$ for $t_1 = 1$

16

FIG 4

A STYLIZED ARTERIAL SEGMENT

Z_{E1}

Z_{E2}

Z_{E3}

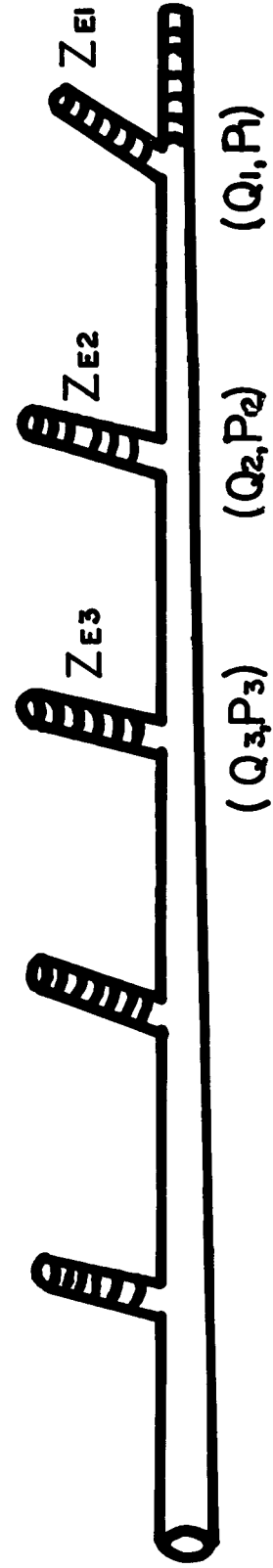(Q_1, P_1)
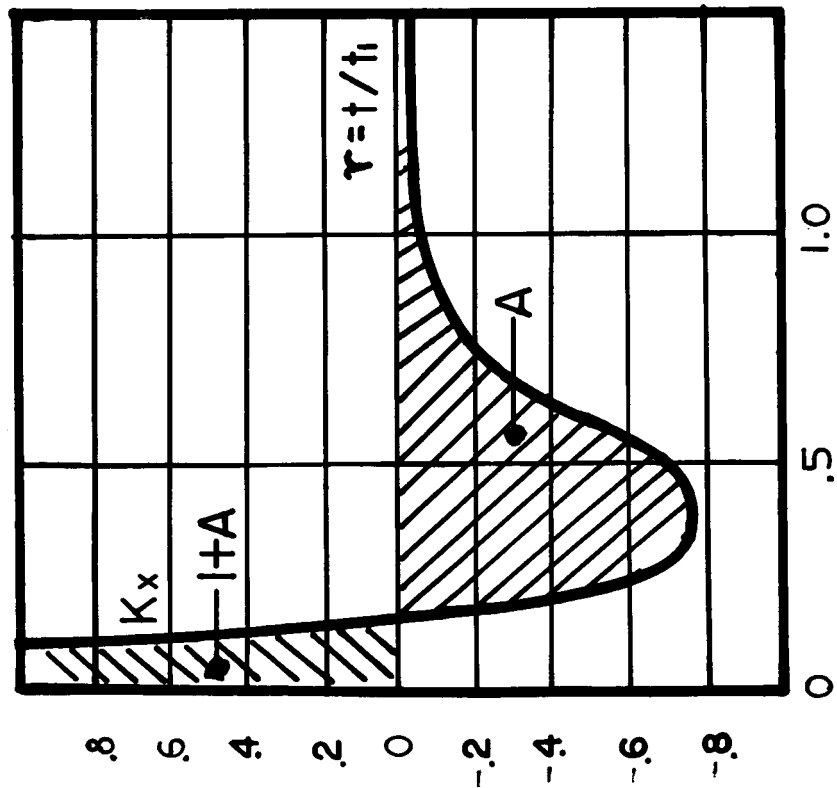
(Q_2, P_2)

(Q_3, P_3)

FIG 5

THE KERNEL K_x

FIG 6

A REPRESENTATIVE ARTERIAL
SEGMENT AT THE LARGE END OF THE
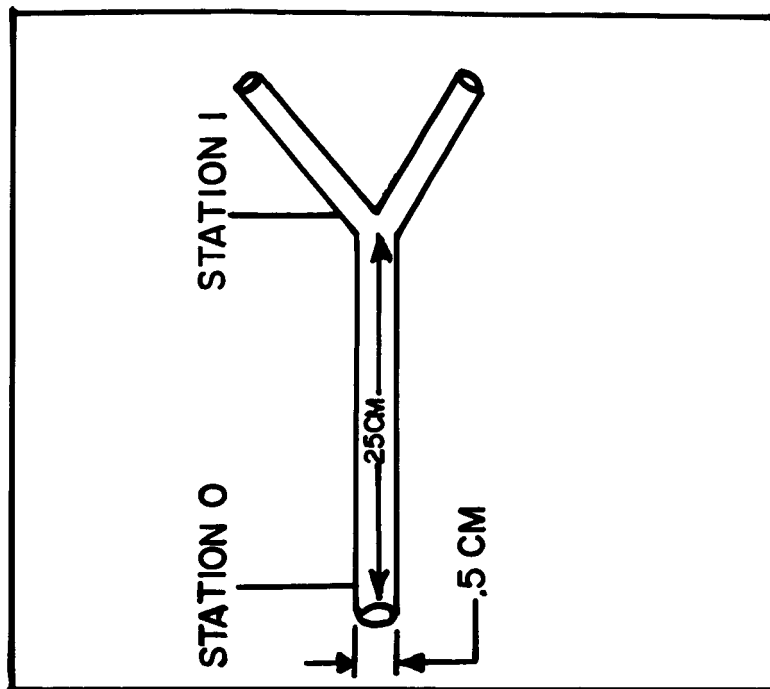SYSTEM

18

FIG 7

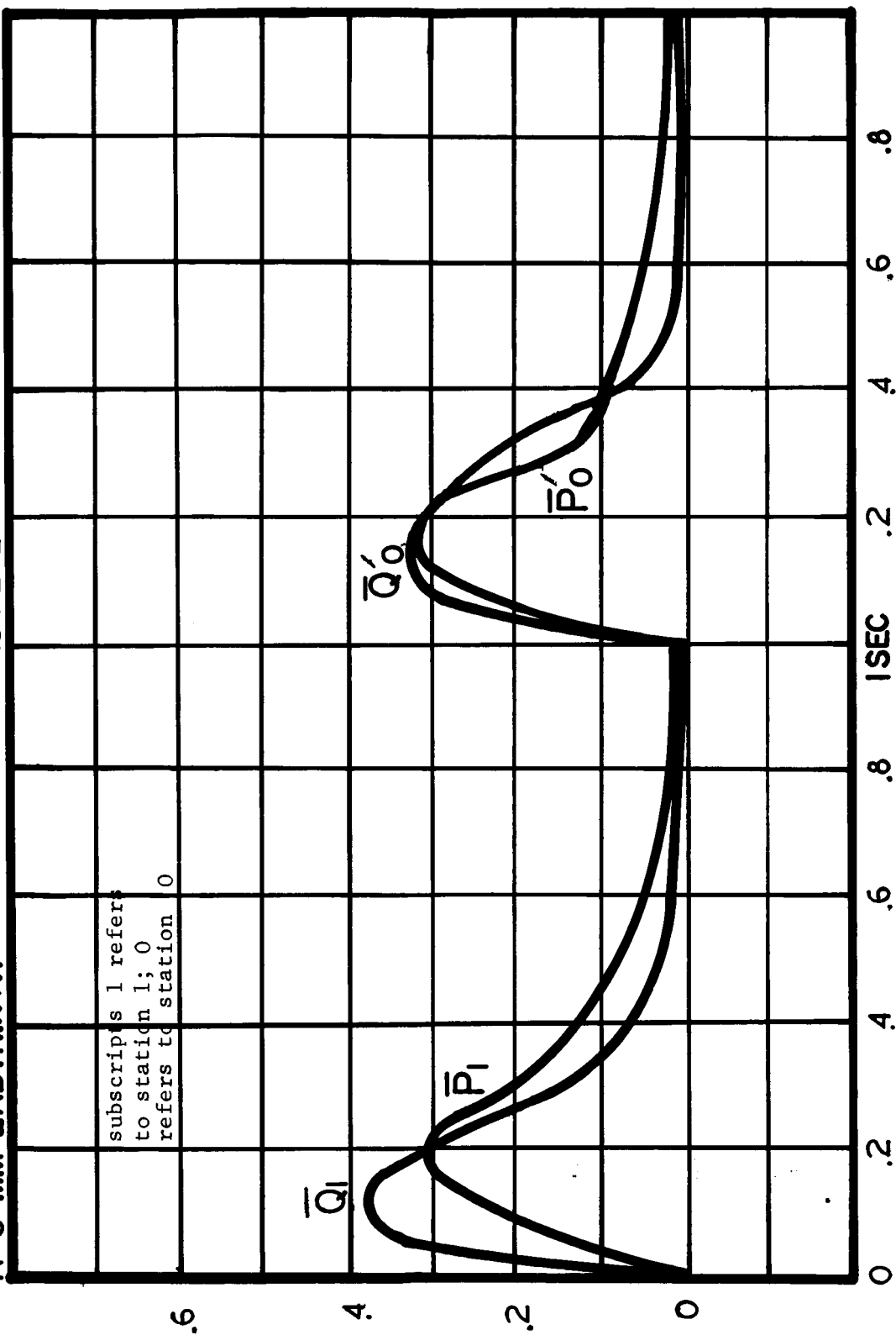### THE IMPEDANCE RELATION FOR A 3 MM LABYRINTH
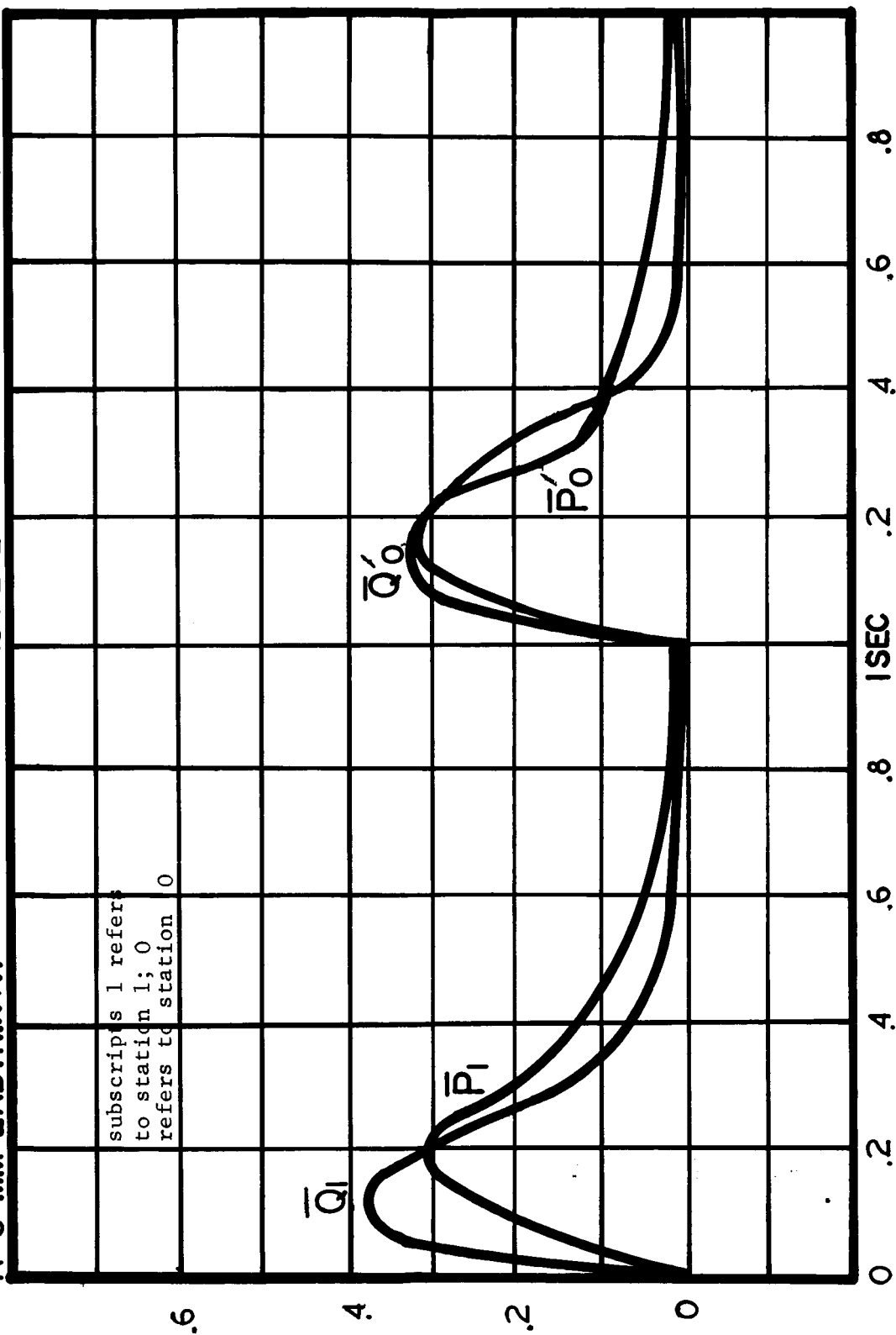
FIG 8

THE IMPEDANCE RELATION IF THE FLUID IS REPLACED BY AN L-C LINE.

subscripts 1 refers to station 1; 0 refers to station 0

$\overline{Q}_1$

$\overline{P}_1$

$\overline{Q}'_0$

$\overline{P}'_0$

ISEC

THE EIGEN VECTOR PAIR INVOLVING $\overline{Q_1}$

THE EIGEN VECTOR PAIR INVOLVING $\overline{P_1}$

THE RESISTIVE LAYERS ACT LIKE LOW
IMPEDANCE SHUNTS CAUSING THE PRESSURE
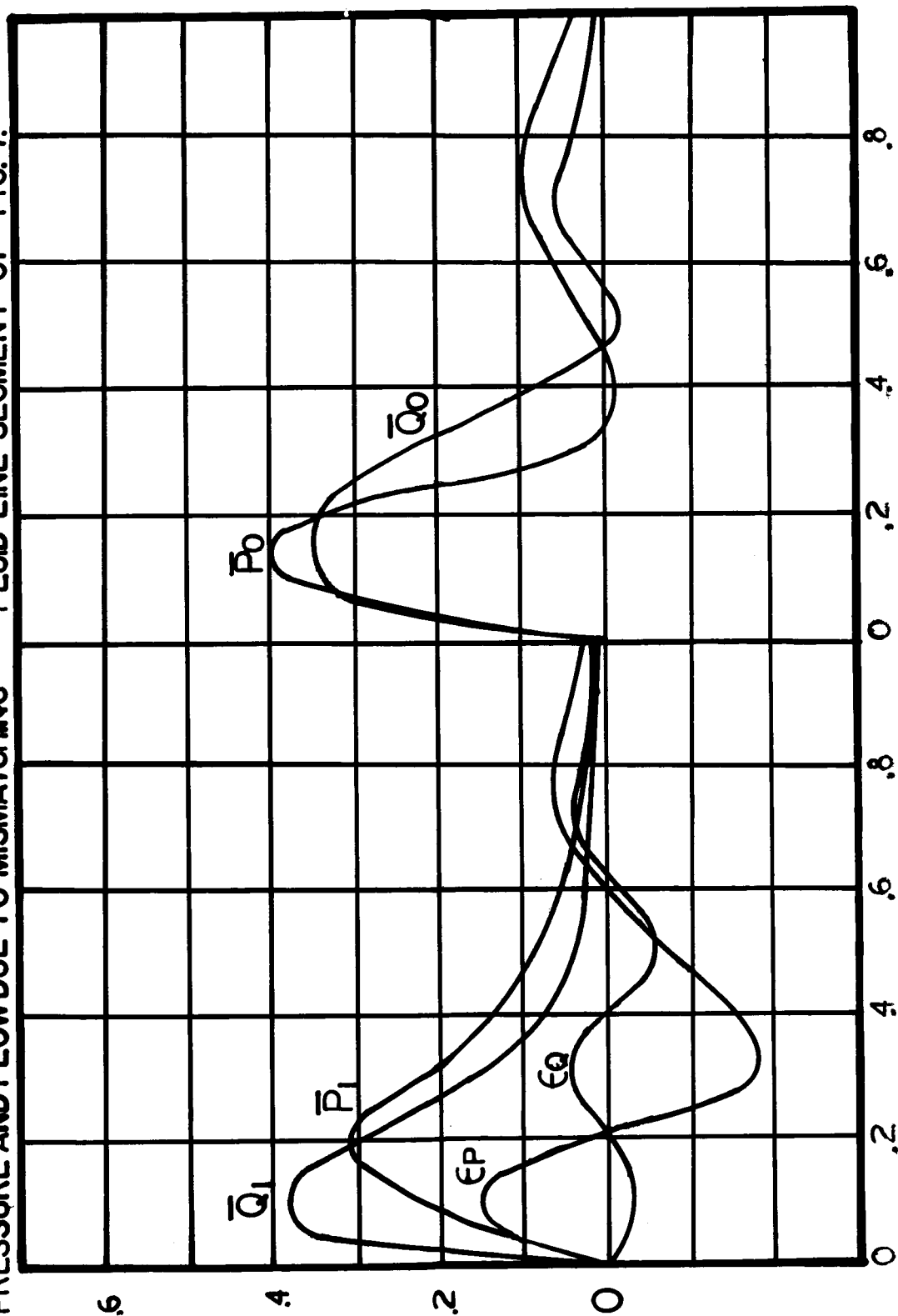PULSE TO OSCILLATE

FIG 10

FIG 9

20
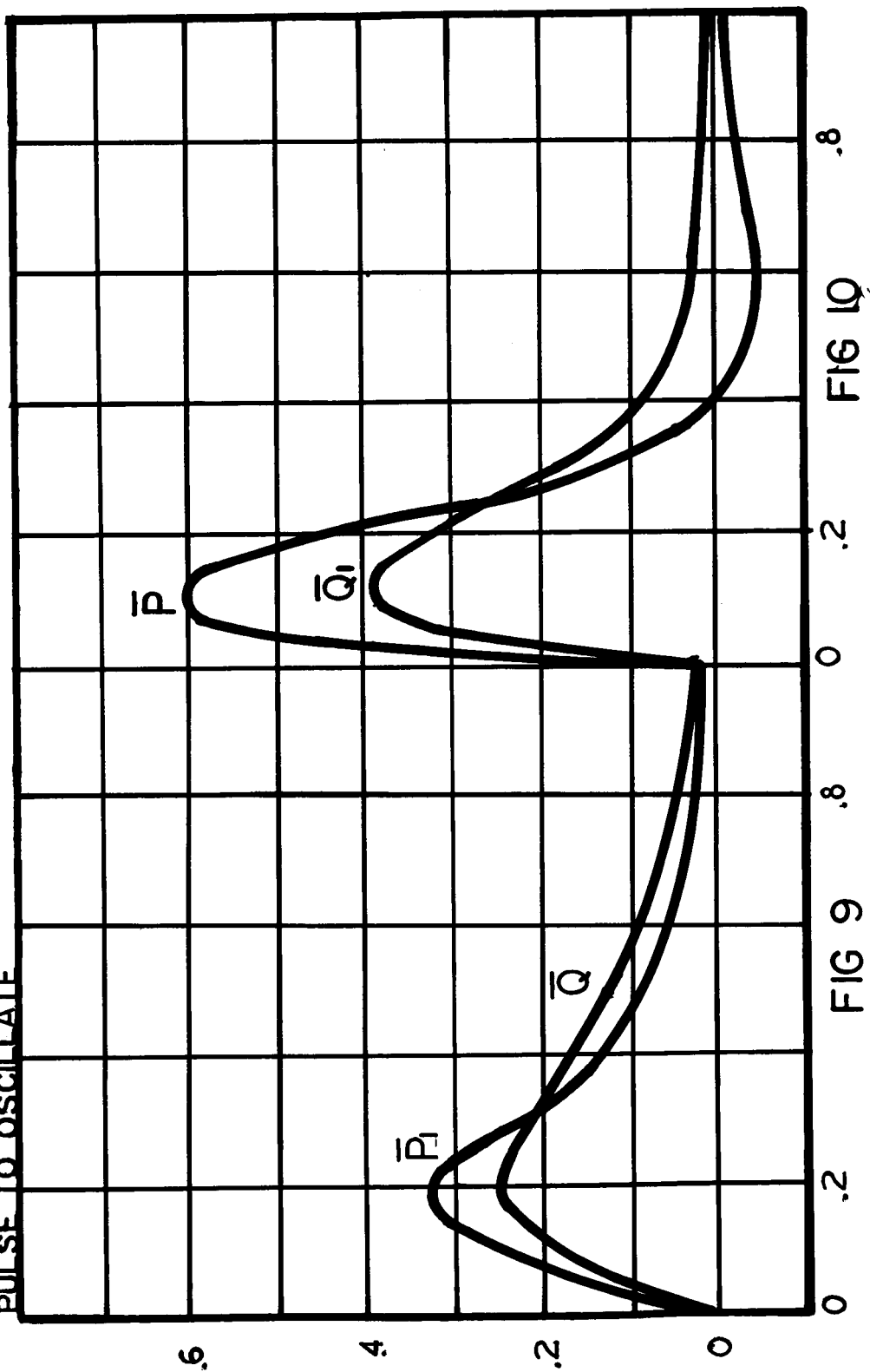
FIG 11

DISTORTION COMPONENTS FOR
PRESSURE AND FLOW DUE TO MISMATCHING

FIG 12

THE IMPEDANCE RELATION FOR THE .5 CM.
FLUID LINE SEGMENT OF FIG. 7.

A GRAPH OF THE EXPONENT INVOLVED IN REPRESENTING PROPAGATIONAL DISTORTION

Real part of $3/2 + \epsilon(z)$

$3/2 + \sqrt{3/2}$

$\sqrt{3/2}$

Imaginary part of $\epsilon(z)$

$z = \omega t_1$
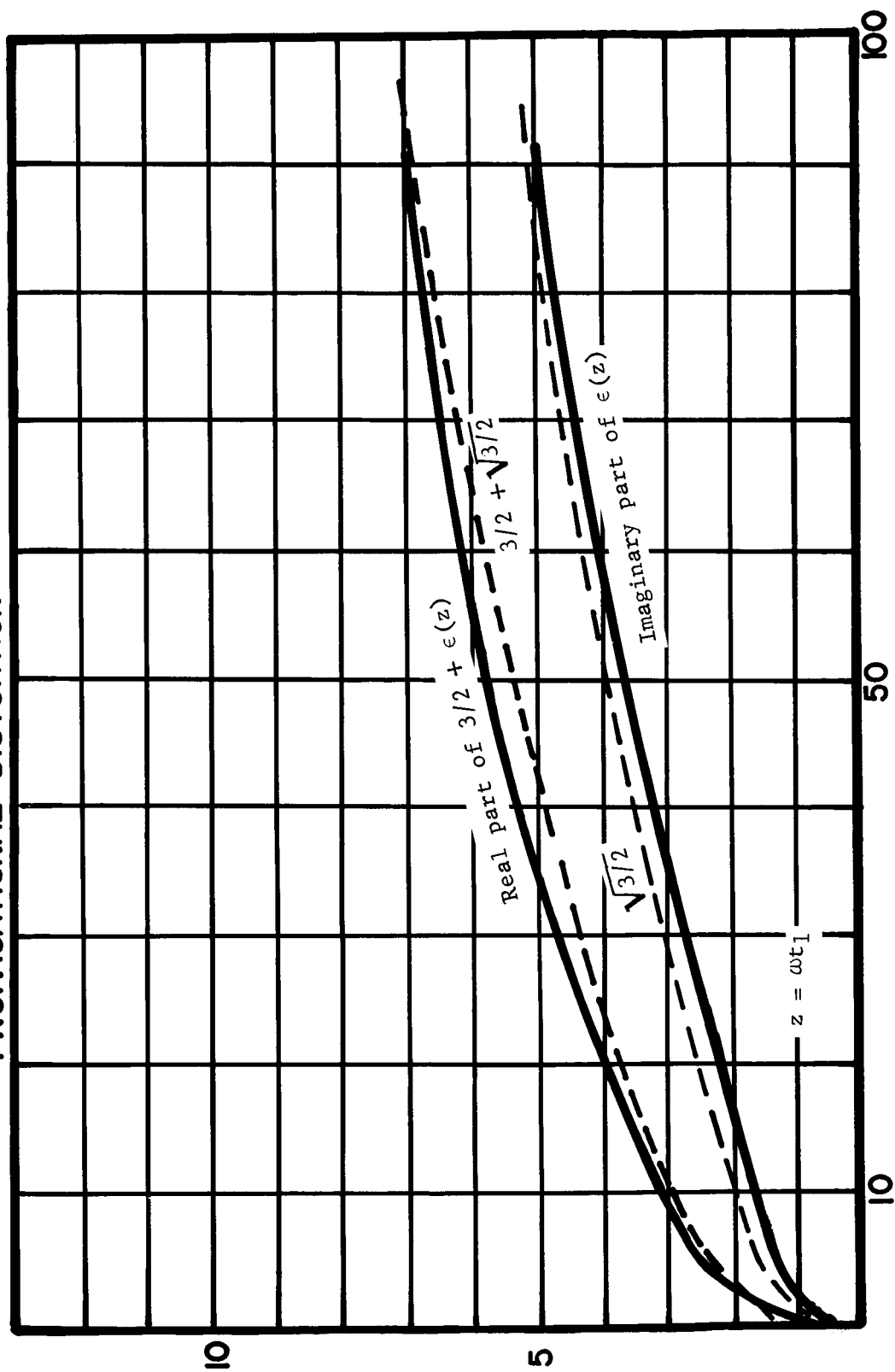
FIG 13

Appendix A

In order to evaluate the kernels K_X, K_{t1}, we let $t_1 = 1$ and express

$$X(z) = \frac{2J_1(\sqrt{-jz})}{\sqrt{jz}\,J_0(\sqrt{-jz})} = \frac{1}{\sqrt{jz}}\,e^{-(\sqrt{jz})}\,\frac{2I_1(\sqrt{jz})}{\sqrt{jz}} \cdot \frac{\sqrt{jz}}{I_0(\sqrt{jz})}\,e^{-(\sqrt{jz})}$$

But

$$F^{-1}\left(e^{-jz}I_1(jz)\right) = \frac{1}{\pi}\,\frac{1-t}{\sqrt{t(2-t)}}\,\left[u(t) - u(t-2)\right]$$

where u is the unit step function. Further,

$$F^{-1}\left(e^{-jz}I_0(jz)\right) = \frac{1}{\pi\sqrt{t(2-t)}}\,\left[u(t) - u(t-2)\right]$$

But, in general

$$F^{-1}\left(\frac{1}{\sqrt{jz}}\,g\,(\sqrt{jz})\right) = \frac{1}{\sqrt{\pi t}}\,\int_0^\infty e^{-u^2/4t}\,h(u)\,du$$

where

$$h = F^{-1}(g).$$

Therefore, on changing variables

$$F^{-1}\left(\frac{1}{\sqrt{jz}}\,e^{-\sqrt{jz}}I_0(\sqrt{jz})\right) = \frac{1}{\sqrt{\pi t}}\,\int_{-\pi/2}^{\pi/2} e^{-(1 + \sin\theta)^2/4t}\,d\theta = h_1(t)$$

Similarly

$$F^{-1}\left(\frac{1}{\sqrt{jz}}\,e^{-\sqrt{jz}}I_1(\sqrt{jz})\right) = \frac{1}{\sqrt{\pi t}}\,\int_{-\pi 2}^{\pi/2} e^{-(1 + \sin\theta)^2/4t}\,\sin\theta\,d\theta = h_2(t),$$

$$F^{-1}\left(\frac{2I_1(\sqrt{jz})\,e^{-\sqrt{jz}}}{jz}\right) = \frac{1}{\sqrt{\pi t}} * h_2,$$

and finally the kernel for X, K_X satisfies

$$K_X * h_1 = \left(\frac{1}{\sqrt{\pi t}}\right) * h_2 \quad.$$

Similarly when K_X is known K_{t1}, represented by $1 - \sqrt{1-X}$ must satisfy

$$\underline{2K_{t1} - K_{t1} * K_{t1} = K_X}$$

$(K_L)_{t1}$ must satisfy

$$(K_L)_{t1} = \left(8 u - u * K_X\right)$$

where u is the unit step function.

We have still to evaluate the kernels K_a.

Now

$$e^{-\epsilon(z)} = e^{-\sqrt{jz}} e^{-\overline{\epsilon}(z)}$$

where $\overline{\epsilon}$ is bounded.

Thus

$$e^{-\overline{\epsilon}(z)} = e^{-\sqrt{jz}} \left(1 - \frac{\epsilon(z)}{1!} + \frac{\epsilon^2(z)}{2!} \quad \cdots \right)$$

where the series converges uniformly in terms of z.

$$\epsilon(z) = \frac{jz}{1-g_{t1}} - jz - \frac{jz}{\sqrt{jz}}$$

$$F^{-1} \frac{1}{\sqrt{jz}} = \frac{1}{\sqrt{\pi\tau}} \quad,$$

if u denotes the unit step function, then the kernel K_ϵ satisfies

$$(1-K_{t1}) * (u * K_\epsilon) = K_{t1} - \left(\frac{1}{\sqrt{\pi\tau}}\right) + K_{t1} * \left(\frac{1}{\sqrt{\pi\tau}}\right)$$

On the other hand the graph of $\epsilon(z)$ is represented in figure 13 as the difference between the dotted lines and solid lines - from which the transform may also be estimated.

The first order effect of K_a is that of

$$F^{-1}(e^{-\sqrt{j}z}) = \frac{1}{2\sqrt{\pi t^3}} e^{-1/4t}$$

which is graphed in figure 1 (where $\alpha = t$ and $t_1 = 1$).

From the curves shown in Figures 1, 2, 3, and 5, any desired kernel may be obtained. For example, if K represents the function K_{t1} for $t_1 = 1$, then for any other value of t,

$$K_{t1}(t) = 1/t_1 \, K(t/t_1)$$

Similarly, for the other kernels. Hence one obtains the desired function by re-scaling.

APPENDIX B

The transform T_a is represented by $K_a = F^{-1}(g_a)$

where

$$g_a(\omega) = e^{-t_o/t_1 \; \epsilon(\omega t_1)} = \left(e^{-\epsilon(\omega t_1)}\right)^{N + r/t_1}$$

where $t_o/t_1 = N + R/t_1$, N an integer and $R < t_1$.

If t_1 is quite small then to/tl_1 may be taken to be the nearest integer because the effect of to/tl on K_a is surely continuous – in fact to/tl will take an integral value somewhere within the tube. In that case K_a is equal to the convolution of $F^{-1}(g_a) = K_{a1}$ with itself N times where $g_{a1}(\omega) = e^{-\epsilon(\omega t_1)}$

then

$$K_{a1}\left(\frac{t}{t_1}\right) = \frac{1}{t_1} \int_o^\infty e^{-\epsilon(z)+jz) \; t/t_1} dz$$

i. e.

$$\left(dK_{a1}\right)_\tau = K_{a1}(\tau)d\tau, \tau = \frac{t}{t_1}$$

Therefore the area under the curve is independent of t_1. It will be seen that the area should be unity, for if a pulse of flow is introduced into an infinite line and the beginning of the line is then closed, then the flow pulse at the source is transformed by K_{a1} into the flow pulse at a station removed so that $t_o/t_1 = 1$ – i.e. so that $\Delta x = ct_1$. The area under the pressure pulse is multiplied by the area under K_{a1}. But the area under the pulse at the new stations is equal to the total flow past that station, as is the area under the original pulse. Therefore these areas must be the same – otherwise some excess volume would be permanently trapped between the two stations, causing a permanent rise in pressure. In figure 1 the solid lines give the real and imaginary part of the exponent of g_{a1} and the curve $\sqrt{jz} + 3/2$ is shown for comparison.

We see from figure 1 that the area under K_a, is nearly all confined to $\alpha < 3$. This means that for tubes of diameter less than 1/3 cm when $t_1 < 1$ the area under K_a is confined to $t < 3$. But because $t_o/t_1 \simeq 1/50$, K_a has little effect on a single segment. Likewise because of small transit time C_a of equation (4) > reduces to the identity I.

While S_a reduces to a transform represented by $\sqrt{YZ}\,\Delta x$ for inputs say of order $e^{-k\sqrt{jz}}$, $k > k_o$, since the series

$$\sum_n \frac{e^{-k\sqrt{jz}}\;(\sqrt{Y(z)Z(z)})^n}{n!}$$

converges uniformily.

Inputs of that order may be thought of as members of the set of all f such that $f = m(K * h)$,

where

$$K = F^{-1}\left(e^{-k\sqrt{jz}}\right) \; ; \int_0^\infty |\,h(t)\,|\,dt = 1.$$

These are characterized as sums of curves at least as "smooth" and as "broad" as

$$F^{-1}\left(e^{-k\sqrt{jz}}\right) = \sqrt{\frac{2}{\pi}}\left(\frac{1}{k^2 t_1}\right)\left(\frac{k^2 t_1}{}\right)^{\frac{3}{2}} e^{-k^2 t1/t}$$

whose features are confined to $t < 3k^2 t_1$.

Therefore equation (2') reduces to

$$\begin{bmatrix} F(Q_{x2}) \\ F(P_{x2}) \end{bmatrix} = \begin{bmatrix} I & Y\Delta x \\ Z\Delta x & |\,I \end{bmatrix} \begin{bmatrix} F(Q_{x1}) \\ F(P_{x1}) \end{bmatrix} \qquad (B1)$$

i. e. to equation (1)

(The eigen values are $\lambda = 1 \pm t_o\,D \pm D\left(\frac{T_{t1}}{1-T_{t1}}\right)$

Consider an artery belonging to one of the levels in this domain (figure 4). The tributary systems are represented dynamically by their impedance functions, $(Z_E)_n$ the recursion relations from terminus to source are

$$F(Q_{n+1}) = F(Q_n) + \left(\frac{A\triangle x}{\rho c^2} j\omega + (Z_{E,})_{n+1}^{-1}\right) F(P_n)$$

$$F(P_{n+1}) = \frac{\rho\triangle x \, jz}{t_1 A(1-X)} F(Q_n) + F(P_n) \qquad (B2)$$

$$X(\omega) = \frac{J_o(\sqrt{-j}z)}{\sqrt{-j}zJ_1(\sqrt{j}z)} \quad , \quad \frac{F(P_1)}{F(Q_1)} = Z_E$$

If the terminal pressure were nearly 0 the first relation would become:

$$Q_1 = Q_o$$

$$F(P_1) = \frac{\rho\triangle x}{t_1 A} \frac{jz}{1-X} F(Q_o)$$

Now $jz/(1-X) \simeq 8$ for $z < 1$ and is smaller in abs. value that $8z$ for $z > 1$.
If

$$Q_o = mK * h$$

where

$$K = F^{-1}(e^{-3\sqrt{jz}}) \quad ; \quad \int_c^\infty |h| dt = 1$$

then one may show

$$\left(F(P_1) - \frac{8\rho\triangle x}{t_1 A} F(Q_o)\right) < me^{-3}$$

for all ω. This means that graphically

$$P_1 = \frac{8\rho\triangle x}{t_1 A} Q_o + \epsilon$$

where ϵ is uniformily small with respect to Q_o. Thus, the terminal relation reduces to Poiseuille's law or something equivalent in character for actual blood flow if one considers the rheology problem.

Further if, in particular, the inputs to an artery consist of sums of curves as smooth and as broad in the previous sense as $F^{-1}(e^{-(1/3)\sqrt{j\omega}})$, which is the typical case in arterial systems below the 3mm size, then first of all, because of attenuation, one expects the situation to improve in all of the tributary systems. Thus if the artery is of such diameter that $e^{-(1/3)\sqrt{j\omega}}$ replaces $e^{-3\sqrt{jt_1\omega}}$ in the previous discussion - i.e., $r^2/\nu = t_1 \simeq 1/81$. Then

inertia may be ignored and the expression $jZ/(1-X)$ in equation (B2) may be replaced by the expression $1/8$. The condition on diameter is $d \leq 1/25$ cm.

We remark parenthetically that from another point of view $8(1-X)/jz$ has an inverse transform $(K_L)_{t1}$ so that multiplying by $jz/8(1-X)$ is equivalent to transforming a function f into $\bar{f}$ where $(K_L)_{t1} * \bar{f} = f$.

We may assume that near the end of the system $\left(Z_E\right)^{-1}_{n+1} \simeq At_1/8\rho\Delta x$. Dividing by the capacitive term, $A\Delta x/\rho c^2$ from equation B2 gives

$$\frac{t_1 c^2}{8\Delta x^2} = \frac{r^2 c^2}{8 \times .035\Delta x^2} \simeq \frac{c^2}{8 \times 50} \geq \frac{5000}{8}$$

As we go to higher levels the capacitance, $A\Delta x/\rho c^2$, grows as the volume while the d.c. admittance grows about linearly with A^K, $1 \leq K \leq 3/2$. Hence the capitance may eventually become significant in a solution to equation (B2) (e.g., consider a Picard's series), but this only when the radius ratio r/r_E is of the order of $\sqrt{5000/8}$, which happens at a diameter of about 1 mm.

Thus the system below the 1/2 mm size appears highly resistive.

For $1/2 < d < 3$ (mm) equation (B2) should still apply, but Z_{E1} is a resistance R_{E1} of the order of N times the terminal resistance of the system, where N is the number of terminal resistors on to tributaries of the system. Thus R_{E1} is bound to be large compared to the local resistance $8\rho\Delta x/t_1 A$ since, as a variable, R_{E1} changes eventually by the area ratio while the local resistance changes with the cube of the radius. (Since $\Delta x/r$ is nearly constant). Also the quantity $A\Delta x/c^2$ is very small compared to $8\rho\Delta x/t_1 A$. This allows the following simplication:

If P_m, Q_m are the pressure and flows at the entrance of a 2-3 mm artery (whose tributaries are essentially of the resistive size), P_E, $Q_E = R_E P_E$ are those at the last tributary, D is the differential operator, L_{t1} is the transform represented by

$$\frac{jz}{8(1-X)} \quad \text{and} \quad A_n = \begin{bmatrix} 0 & \dfrac{A_n \Delta x_n D}{\rho c^2} + \dfrac{1}{R_{En}} \\ \dfrac{8\rho\Delta x_n}{t_{1n} A_n} L_{t1n} & 0 \end{bmatrix}$$

Then the relation among these is given by Picard's series and will be written in informal symbolism as

$$
\begin{bmatrix} Q_m \\ P_m \end{bmatrix} = \begin{bmatrix} e^{\Sigma A_n} \end{bmatrix} \begin{bmatrix} Q_E \\ R_E & Q_E \end{bmatrix}
$$

The simplification is that the series converges so rapidly that this expression becomes essentially

$$
\begin{bmatrix} Q_m \\ P_m \end{bmatrix} \quad \begin{bmatrix} I + \sum_n A_n \end{bmatrix} \begin{bmatrix} Q_E \\ R_E & Q_E \end{bmatrix}
$$

or

$$
\begin{bmatrix} Q_m \\ P_m \end{bmatrix} = \begin{bmatrix} 1 & V/\rho c^2 D + \sum_n 1/R_{En} \\ \sum_n \dfrac{8\rho \Delta x_n}{t_{1n} A_n} & 1 \end{bmatrix} \begin{bmatrix} Q_E \\ Q_E & R_E \end{bmatrix}
$$

where V is the volume of the system.

Therefore the driving point impedance of a 3 mm arterial system given by

$$
\left(\frac{vD}{\rho c^2} + \sum 1/R_{En} \right) P_m = \left(1 + \sum \frac{R_n}{R_{E1}} L_{t1} \right) Q_m \tag{B3}
$$

where

$$
R_n = \frac{8\rho \Delta x_n}{t_{1n} A_n}
$$

In representative figures

$$
10^{-5} (D+1) P_m = (1+L) Q_m
$$

where L^{-1} represented by a kernel of area a, $10 < a < 200$. Thus, these tubes look like simple lumped R-C elements.

REFERENCES

1. Ahlfors, L. V., COMPLEX ANALYSIS, AN INTRODUCTION TO THE THEORY OF ANALYTIC FUNCTIONS OF ONE COMPLEX VARIABLE, McGraw-Hill, N. Y., 1953.

2. Attinger, E. O., Ed., PULSATILE BLOOD FLOW, McGraw-Hill, N. Y., 1964.

3. Attinger, E., Anne A., "Simulation of the Cardiovascular System," Annals N. Y. Acad. Sci. 128, 810, 1966.

4. Brown, F. T., "Transactions of the ASME," Journal of Basic Engineering 84, p. 547, 1962.

5. Fich, S., Welkowitz, W., and Hilton, R., "Pulsatile Blood Flow in the Aorta," Biomedical Fluid Mechanics Symposium, Fluids Eng. Div., ASME, 34, 1966.

6. Green, H., "Circulatory System: Physical Principles," in O. Glasser, MEDICAL PHYSICS, Vol. 2, 2, 228, 1950.

7. Hobson, E. W., THEORY OF FUNCTIONS OF A REAL VARIABLE, Dover, N. Y., 1957.

8. Iberall, A. S., "Attenuation of Oscillatory Pressures in Instrument Lines," Jour. of Research, National Bureau of Standards, 15, July 1950 R.P. 2115.

9. Iberall, A. S., "Study of the General Dynamics of the Physical-Chemical Systems in Mammals," NASA CR-129, Oct. 1964.

   Cardon, S. Z., Jayne, T., "General Dynamics of the Physical-Chemical Systems in Mammals," Dec. 1965 Interim Report. Available from General Technical Services, Inc., Upper Darby, Penna. 19082.

10. Iberall, A. S., "Anatomy and D.C. Char. of the Arterial System with an Introduction to Its A.C. Char.," NASA CR-770, May, 1967.

11. Intaglietta, M., Zweifach, B., "Indirect Method of Measurement of Pressure in Blood Capillaries," Circ. Res. 19, 199, 1966.

12. Jaeger, G., Westerhof, N., Noordergraaf, A., "Oscillatory Flow Impedance in Electrical Analog of Arterial System . . .," Circ. Res. 16, 121, 1965.

13. Karreman, G., "The Resonance of the Arterial System," Bull. Math. Biophysics, 16, 159, 1954.

14. Mall, F., Konig, Sachs, Gessell, d. Wiss, Abh. d. Math. Cl. 14, 1888.

15. McDonald, D., BLOOD FLOW IN ARTERIES, Arnold, 1960.

16. McDonald, D. A. and Taylor, M. G., "The Hydrodynamics of the Arterial Circulation," Progress in Biophysics, 9, 105, 1959.

17. Noordergraaf, A., Verdouw, P. D., Van Brummelen, A. G. W., and Wiegel, F. W., "ANALOG OF THE ARTERIAL BED:" "PULSATILE BLOOD FLOW," E. O. Attinger, Ed. McGraw-Hill, N. Y., 1964.

18. Oberhettinger, F., TABELLEN ZUR FOURIER TRANSFORMATION, Springer, Berlin, 1957.

19. Skalak, R., and Stathis, T., "A Porous Tapered Elastic Tube Model of a Vascular Bed," Biomechanics, ASME Symposium, 1966.

20. Sneddon, I. A., FOURIER TRANSFORMS, McGraw-Hill, N. Y., 1951.

21. Suwa, N., et al, "Estimation of Intravascular Blood Pressure Gradient by Mathematical Analysis of Arterial Casts," Tohoku J. of Exper. Med., 79, 168, 1963.

22. Taylor, M. G., "Use of Random Excitation and Spectral Analysis in the Study of Frequency Dependent Parameters of the Cardiovascular System," Circ. Res., 18, 5, 585, 1966.

23. Taylor, M. G., "The Input Impedance of an Assembly of Randomly Branching Elastic Tubes," Biophysical Journal, 6, 29, 1966.

24. Weinberg, L., NETWORK ANALYSIS AND SYNTHESIS, McGraw-Hill, N. Y., 1962.

25. Witzig, K., Inaug. Diss., Univ. of Bern, Wyss, Bern, 1914.

26. Womersley, J., W. A. D. C. Tech. Rep. 50-614, 1958.